33rd Annual International Conference of the IEEE EMBS
Boston, Massachusetts USA, August 30 - September 3, 2011

A Computer-Aided Method for Automatic Localization and Thickness Measurement of Peritoneum in Ultrasound Images

Yu-Shan Lin, Tsung-Chun Lee, Hsuan T. Chang, *Senior Member, IEEE,* Syu-Jyun Peng, Jenq-Wen Huang, Hsiu-Po Wang, Chung-Wen Hung

***Abstract*—This paper presents a method of automatically measuring peritoneum thickness in ultrasound images. In our previous work, a method of manually selecting the region of interest (ROI) area has been developed. To achieve an automatic ROI area selection, two phases: Gaussian high-pass filtering and bilateral filtering, are used in the proposed method. In the bilateral filtering phase, the ultrasound image is enhanced for obtaining more details of the peritoneum so that probable areas can be extracted. In the other phase, the ultrasound image is processed with a Gaussian high pass filter, and the result is used to locate the precise area of peritoneum in the first phase result. The experimental results show that the proposed method has high accuracy and fast processing speed in determining the peritoneum area and its thickness distribution.**

I. Introduction

THE ultrasound imaging technology has been widely used for a long time. It provides the medical personnel a non-invasive way to detect the information of human body. Since the ultrasound imaging technology can provide the reliable message, the research of ultrasound images analysis on various parts of the body has become an important research, especially the abdomen. Some computer-aided diagnosis (CAD) tool for ultrasound image has been developed that help the doctor in the diagnosis of patients.

There have been many previous studies in the ultrasound image segmentation. Belaid *et. al.* segment ultrasound images by considering Phase-based level set [1]. Takemura *et. al.* apply automated segmentation method of breast tumors on ultrasonic images [2]. Gutierrez *et. al.* segment the cerebellum of fetuses on 3D ultrasound images [3]. Schneider *et. al.* apply 3D ultrasound images segmentation on mitral annulus [4]. Rocha *et. al.* apply ultrasound images segmentation on carotid [5]. Tran and Rohling detect lumbar anatomy of human subjects on ultrasound images [6]. Chang *et. al.* apply ultrasound images segmentation on thyroid [7]. Shrimali *et. al.* apply and improve ultrasound images segmentation for fetal biometry [8]. Chiu *et. al.* analyze the variability dependence on signal difference and boundary orientation on 3D carotid ultrasound segmentation [9]. Slabaugh *et. al.* segmentation ultrasound images by considering the statistical region [10].

Respective to different parts of the human body, there are many types of ultrasound imaging. In our previous work, we have developed a CAD methodology to manually detect the peritoneum and then automatically measure the thickness. According to doctor's experience, the peritoneal thickness of a patient after undergoing dialysis for a long time might change. The CAD in this study can support doctor in investigating the different effects on the peritoneum thickness between peritoneal dialysis patients and normal person [11].

In our previous study [12], the area of peritoneum has to be manually marked down. As shown in Fig. 1(a), the area circled in the blue line is the manually selected peritoneum area. Next, the precise area is measured with the aid of our proposed algorithm, as shown in Fig. 1(b) with red boundary lines. Finally, the peritoneum thickness distribution can be calculated. However, the method requires manual marking, which costs extra manpower and time. To further improve this method, we develop a method using bilateral filtering to enhance the ultrasound image so the probable peritoneum areas can be automatically detected.

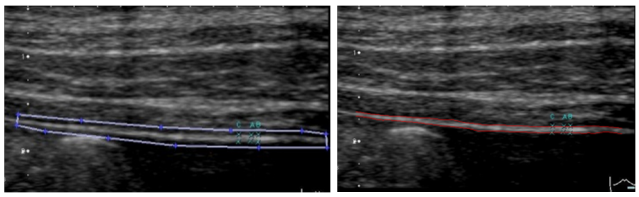

(a) (b)

Fig. 1. The probable peritoneum areas depicted by (a) manual remark; (b) using the proposed computer algorithm.

II. Method

A. Overview

The main idea of the method is to combine the ROI area obtained from the bilateral filtering and the Gaussian high pass filter (GHPF) result to determine the peritoneum. Figure 2 shows the block diagram of the system.

B. Bilateral filtering phase

Since the values of the neighboring pixels on an ultrasound image (which is grayscale) are too close to each other, it is not easy to precisely define the correct area of the peritoneum. To solve this problem, the bilateral filtering technique [13] is applied here to enhance the image.

Manuscript received March 24, 2011. This work was supported in part by the National Science Council under the contract number NSC 99-2221-E-224-004. The authors also want to thank National Taiwan University Hospital and College of Medicine for providing the ultrasound images.

Hsuan T. Chang, Yu-Shan Lin, and Chung-Wen Hung are with Department of Electrical Engineering, National Yunlin University of Science & Technology (YunTech), Taiwan (886-5-5342601 ext. 4263, htchang@yuntech.edu.tw)

Tsung-Chun Lee, Jenq-Wen Huang, and Hsiu-Po Wang are with Department of Internal Medicine, National Taiwan University Hospital and College of Medicine, National Taiwan University, Taiwan (tsungchunlee@gmail.com)

Syu-Jyun Peng is with Department of Electrical Engineering, National Central University, Taiwan (blue.year@msa.hinet.net)

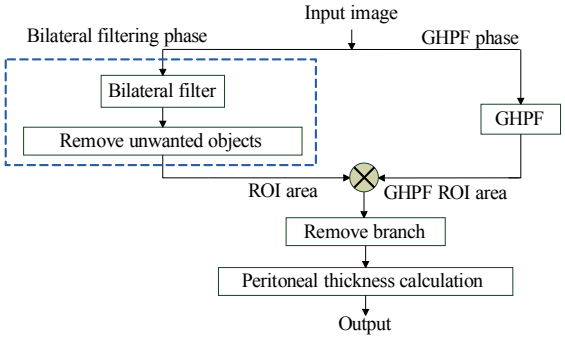

Fig. 2. The overview of the proposed method.

The principle of bilateral filtering is based on the Gaussian blur and anisotropic diffusion [14]. It uses the Gaussian smoothing in the spatial domain and the intensity domain in images. The bilateral filtering operation can be expressed as:

$$J_S = \frac{1}{k(s)} \sum_{p \in \Omega} f(p-s) g(I_P - I_S) I_P \,, \qquad (1)$$

where f represents the spatial domain of the Gaussian smoothing filter function, g represents the intensity domain of the Gaussian smoothing filter function, J is the result after bilateral filtering, p is the center pixel, s is the pixels around the center, Ω are pixels of the image, and I is the intensity of the pixel. In addition, k is a normalization function:

$$k(s) = \sum_{p \in \Omega} f(p-s) g(I_P - I_S) \quad . \qquad (2)$$

After the image is processed by the use of a bilateral filter, the detail image can be extracted. The detail image D is expressed as:

$$D = U - B, \qquad (3)$$

where U denotes the original image and B represents the filtering result, also called the base image. Figure 3 shows the enhancement process. The process can be expressed as the steps shown as the following equations:

$$D_1 = U - B_1, \qquad (4)$$

$$E_1 = U + D_1 * r1, \qquad (5)$$

$$D_2 = E_1 - B_2, \qquad (6)$$

$$E_2 = U + D_1 * r2 + D_2 * r3, \qquad (7)$$

where E_1 and E_2 represent the 1st and 2rd enhanced images, D_1 and D_2 are the 1st and 2rd detail images, B_1 and B_2 are the 1st and 2rd base images, $r1$, $r2$, $r3$ denote the three gain ratios of the detail image. The gain ratios can adjust the enhance level by folding up the detail image. Here $r1$ usually set as 100, $r2$ set as 2 and $r3$ set as 1. Figure 4 shows the comparison of the original, detail, and base images. The image enhancement results are shown on Fig. 5.

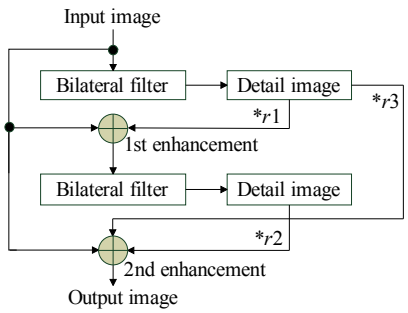

Fig. 3. The procedure of image enhancement using bilateral filtering.

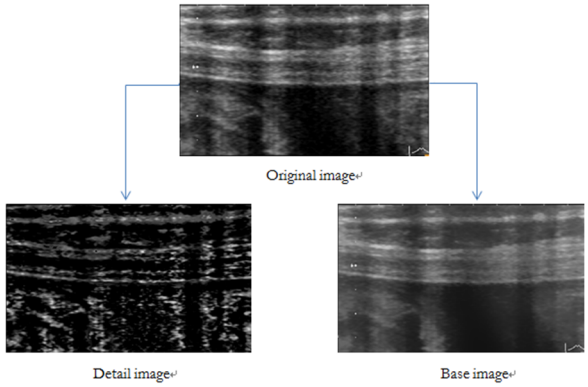

Fig. 4. The comparison between the original, detail, and base images.

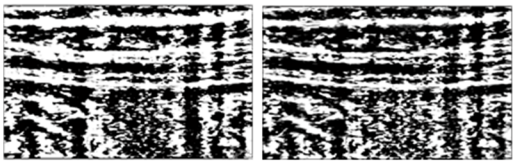

(a) (b)

Fig. 5. The results of the (a) 1st enhancement; (b) 2nd enhancement.

The next step is to choose the threshold value to for binarization image. The binary image can be used to label and remove the objects that do not belong to the peritoneum. The specific steps are shown as follows:

Step 1: Assess the size of each object.

$$A(n) = \sum_{i=0}^{u} \sum_{j=0}^{v} (L(i,j) = n), \qquad (8)$$

where n is the object index, L is a u x v binary image after labeling, and A is the sum of each object.

Step 2: Assess the aspect ratio of each object

$$R(n) = \frac{length\ of\ each\ object}{width\ of\ each\ object} \,. \qquad (9)$$

Step 3: Remove the objects that have few size ratio objects.

$$\begin{cases} L_n(i,j) = 1 & \text{if } A(n) > \alpha \ \vee \ R(n) > \beta \\ L_n(i,j) = 0 & \text{else} \end{cases}, \qquad (10)$$

where α is the threshold value of the size, β is the threshold value of the aspect ratio. In our experimental, α and β set as 2500 and 4, respectively.

Step 4: Use the linear structuring element in the morphological dilation to connect the objects in the horizontal direction.

Step 5: Remove the objects that are shorten than certain lengths after relabeling.

$$\begin{cases} L_{n2}(i,j) = 1, & \text{if length}(n2) > \delta \\ L_{n2}(i,j) = 0, & \text{else} \end{cases}, \qquad (11)$$

where n_2 is the object after relabeling and δ is the length of each object. In our experimental, δ set as 80% of the image length.

Step 6: Select the object closest to the image bottom.

According to doctor's experiences, the long strip object closest to the bottom of the image usually is the peritoneum area. Consider the relationship between the object and binary images. The bitwise AND operation can be applied to the images of the bilateral filter's ROI area. This can be denoted as:

$$M = O \otimes b, \qquad (12)$$

where M is the ROI area obtained in the bilateral filter phase, O is the object that has been chosen as the peritoneum area, and b is the binary image after the image enhancement. The results of each step (from the binary image to the selection of the peritoneum area) are shown in Figs. 6(a)-6(e).

C. GHPF phase

The GHPF is widely used to analyze the image information. It can be denoted as:

$$G(x,y) = U\left[1 - \boldsymbol{e}^{\frac{-(x^2+y^2)}{2\sigma^2}}\right], \quad (13)$$

where U is the ultrasound image and G is the filtered result and σ is the standard deviation of the Gaussian distribution. The result is shown in Fig. 7(a). The GHPF result has more precise areas of peritoneum, but it is hard to segment them all. To extract the GHPF ROI area, the bitwise AND operation is applied to the results of GHPF and bilateral filtering phase. This can be expressed as:

$$H = G \otimes M, \quad (14)$$

where H is the GHPF ROI area, G is the GHPF result, and M is the ROI area in the bilateral filtering phase. The results is shown in Fig. 7(b).

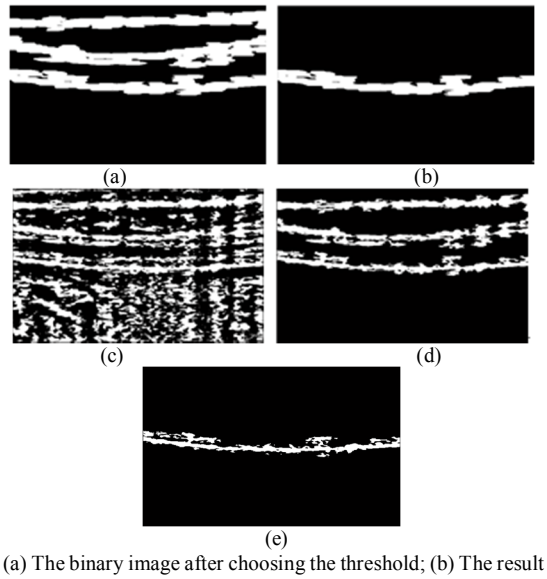

Fig. 6. (a) The binary image after choosing the threshold; (b) The result of the binary image after removal of the object that have less size and length; (c) The expansion of image morphology result; (d) Select the object closest to the bottom of the image; (e) The ROI area on bilateral filter phase.

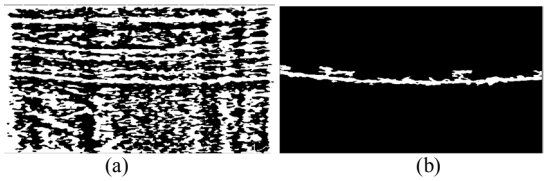

Fig. 7. (a) The GHPF result; (b) The extracted GHPF ROI area.

D. Removing branches

The extracted ROI areas still have some branches that are not needed, as shown on Fig. 8(a). The thickness of peritoneum will be affected by branches, especially the larger branches. In this phase, the branches will be removed, with the result shown in Fig. 8(b).

The peritoneal is observed as strip-shaped. It means that the connection to the strip branch can be broken if the triple connection points can be found. To detect the triple connection point, the morphological thinning operation is required. The thinning result of the area is shown on Fig. 9(a). To detect the triple connection point, a simple way is to measure the neighbors of each pixel of the ROI area after thinning. The detection of connecting triple point of each pixel can be expressed as:

$$\begin{aligned} T = {} & H_{thin}(u-1,v-1) + H_{thin}(u,v-1) \\ & + H_{thin}(u-1,v) + H_{thin}(u+1,v-1) \\ & + H_{thin}(u-1,v+1) + H_{thin}(u+1,v) \\ & + H_{thin}(u,v+1) + H_{thin}(u+1,v+1) \end{aligned} \quad (15)$$

$$\begin{cases} H_{thick}(u,v) = H_{triple} & \text{if } T = 3 \\ H_{thick}(u,v) \neq H_{triple} & \text{else} \end{cases}, \quad (16)$$

where the T is the measure of the neighbors and H_{thick} is the pixel on the thinning area. The result of triple connection points is shown on Fig. 9(b).

Figure 10(a) shows that the junction points are almost located above or below the triple connection point. To break the connection, the junction points must be removed. The process of each connecting triple point is expressed as:

$$\begin{cases} H_{thick}(u,v-1) = 0, & \text{if } H_{triple}(u,v-1) = 1 \\ H_{thick}(u,v+1) = 0, & \text{if } H_{triple}(u,v+1) = 1 \end{cases}, \quad (17)$$

where H_{triple} is the triple connecting point on the thinning area. The result with the junction points removed is shown in Fig. 10(b). After the branch removal step, the ROI area is more precise and smooth.

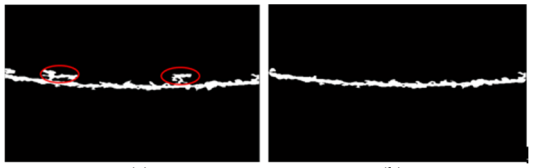

Fig. 8. (a) The red circles denote redundant branches; (b). Removal of the branches.

E. Peritoneal thickness calculation

Finally, after obtaining the ROI area of the peritoneum, the thickness can be determined. Figure 11shows that the thickness result is plotted as the curve to assist doctors to analyze the data on peritoneal dialysis patients.

III. EXPERIMENTAL RESULTS

In our experiments, five cases are used to test the method. The ultrasound image is of size 716*537. The computer specification is as follows: CPU: AMD Phenom II X4 905e, 2500 MHz, RAM: DDR2 4G. The simulation is implemented using MATLAB 2010a. For each image, the processing time costs about 2-3.5 seconds and the test results are shown in Table1. The proposed method can detect the correct peritoneum area when the image is clear. However, if the peritoneum is not clear in the image, the peritoneum area could be misidentified. It can be improved by changing the threshold values on the image binarization or the length parameter. An example about the incorrect detection and

using a better threshold of the length to obtain the correct result is shown in Figs. 12(a) and 12(b).

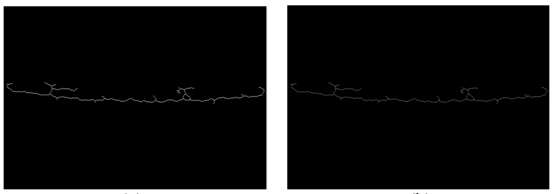

(a) (b)

Fig. 9. (a) The ROI area after thinning morphological operation; (b) The triple point shown on thinning ROI area.

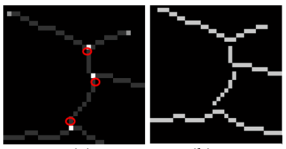

(a) (b)

Fig. 10. (a) Junction points shown on red circle areas. (b) The result of junction points after removing and breaking the junctions.

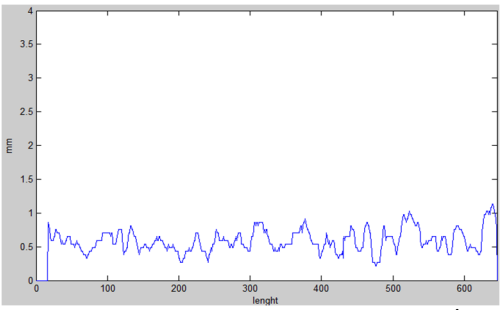

Fig. 11. The thickness distribution of the measured peritoneum.

TABLE1
Test result of the proposed method.

	Images in each medical record	Peritoneal found	Accuracy	Average peritoneal thickness
CASE1	11	9	72.7%	0.55 mm
CASE2	8	8	100%	0.605 mm
CASE3	8	8	100%	0.587 mm
CASE4	8	8	100%	0.547 mm
CASE5	9	8	88%	0.538 mm
Total	44	40	90.9% (in average)	

VI. Conclusion

This paper presents a CAD method that allows the user to automatically measure the thickness of peritoneum in ultrasound images. The method combines the technique of the bilateral filtering and Gaussian high-pass filtering. The major work on bilateral filtering phase is to enhance the image so the peritoneum can be segmented. Combined with the GHPF result, the algorithm can extract the ROI area of peritoneum more precisely. After removing the branches in ROI area, the thickness can be calculated and the distribution curve can be displayed for further analysis. The experimental results show that the method has good accuracy and fast processing time.

In our future work, a better assessment on the threshold values and selects the ROI area is expected. Another focus for the future work is to further improve the method so it can also be applied to ultrasound images for different parts of the body.

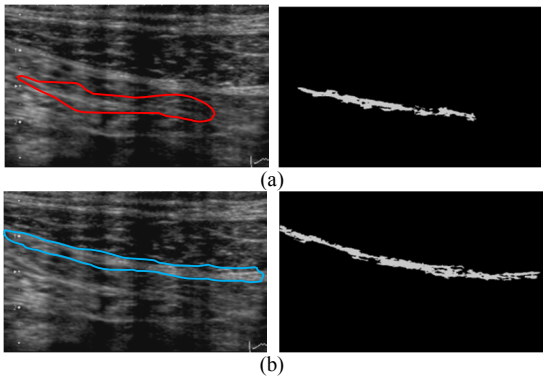

(a)

(b)

Fig. 12. (a) The mistake case, the red circle shows the error ROI area found by the proposed method; (b) After fixing the threshold of the length, the ROI area can be correctly found in blue circle.

References

[1] A. Belaid, D. Boukerroui, Y. Maingourd, and J.F. Lerallut, "Phase-based level set segmentation of ultrasound images," *IEEE Transactions on Information Technology in Biomedicine*, 2011, pp. 138 - 147.

[2] A. Takemura, A. Shimizu, and K. Hamamoto, "A cost-sensitive extension of AdaBoost with Markov random field priors for automated segmentation of breast tumors in ultrasonic images," *Int J Comput Assist Radiol Surg*, 2010, pp. 537–547.

[3] B. Gutierrez, C.F. Arambula, H.M. Guzman, and J.A. Benavides-Serralde, "Automatic segmentation of the cerebellum of fetuses on 3D ultrasound images, using a 3D Point Distribution Model, " *Conf Proc IEEE Eng Med Biol Soc*, 2010 , pp. 4731-4734.

[4] R.J. Schneider, D.P. Perrin, N.V. Vasilyev, G.R. Marx, P.J. del Nido, and R.D. Howe, "Mitral annulus segmentation from 3D ultrasound using graph cuts," *IEEE Trans Med Imaging*, 2010 , pp. 1676-1687.

[5] R. Rocha, A. Campilho, J. Silva, E. Azevedo, and R. Santos, "Segmentation of ultrasound images of the carotid using RANSAC and cubic splines," *Comput Methods Programs Biomed*, 2011, pp. 94-106.

[6] D. Tran and R.N. Rohling, "Automatic detection of lumbar anatomy in ultrasound images of human subjects," *IEEE Trans Biomed Eng*, 2010, pp. 2248-2256.

[7] C.Y. Chang, Y.F. Lei, C.H. Tseng, and S.R. Shih, "Thyroid segmentation and volume estimation in ultrasound images," *IEEE Trans Biomed Eng*, 2010, pp. 1348-1457.

[8] V. Shrimali, R.S. Anand, and V. Kumar, "Improved segmentation of ultrasound images for fetal biometry, using morphological operators," *Conf Proc IEEE Eng Med Biol Soc*, 2009, pp. 459-462.

[9] B. Chiu, A. Krasinski, J.D. Spence, G. Parraga, and A. Fenster, "Three-dimensional carotid ultrasound segmentation variability dependence on signal difference and boundary orientation," *Ultrasound Med Biol*, 2010, pp. 95-110.

[10] G. Slabaugh, G. Unal, M. Wels, T. Fang, and B. Rao, "Statistical region-based segmentation of ultrasound images," *Ultrasound Med Biol*, 2009, pp. 781-795.

[11] T.-C. Lee, J.-Y. Yang, H.-P. Wang, T.-J. Tsai, and Y. Yang, "Peritoneal thickening is not inevitable in long-term peritoneal dialysis and is associated with peritoneal transport characteristics: a two-centre sonographic study," *Nephrol Dial Transplant,* 2008, vol. 23, pp. 1005–1010.

[12] S.-J. Peng, T.-C. Lee, J.-W. Huang, H.-T. Chang, and J.-Z. Tsai, "Computer-aided diagnosis in ultrasound thickness of peritoneum is highly correlated with physician's manual measurement in peritoneal dialysis patients," *International Forum on Medical Imaging in Asia*, Okinawa, Japan, 2011, pp. 171–172.

[13] C. Tomasi and R. Manduchi, "Bilateral filtering for gray and color images," *IEEE International Conference on Computer Vision*, 1998, pp. 67-75.

[14] P. Perona and J. Malik, "Scale-space and edge detection using anisotropic diffusion," *Proceedings of IEEE Computer Society Workshop on Computer Vision*, 1987, pp. 16–22.